POLYMERS FOR ADVANCED TECHNOLOGIES
Polym. Adv. Technol. 2006; **17**: 764–771
Published online 23 August 2006 in Wiley InterScience (www.interscience.wiley.com). DOI: 10.1002/pat.752

PAT

Preparation and characterization of poly(ethylene terephthalate)/clay nanocomposites by melt blending using thermally stable surfactants†

Marius C. Costache[1], M. J. Heidecker[2], E. Manias[2] and Charles A. Wilkie[1]*

[1]Department of Chemistry, Marquette University, PO Box 1881, Milwaukee, WI 53201, USA
[2]Department of Materials Science & Engineering, Penn State University, University Park, PA 16802, USA

Received 5 December 2005; Revised 4 March 2006; Accepted 24 March 2006

Poly(ethylene terephthalate) (PET)/clay nanocomposites were prepared by melt blending and their morphologies and properties were investigated through X-ray diffraction, bright field transmission electron microscopy, thermogravimetric analysis and cone calorimetry. Three clays were comparatively studied—montmorillonite, hectorite and magadiite—all organically modified with thermally stable surfactants developed in this laboratory. Two such organic modifications were investigated, alkyl-quinolinium surfactants and vinylbenzyl-ammonium containing copolymers; both organic modifications combine high enough degradation temperature to allow for melt processing with PET, and also favorable thermodynamics for nanocomposite formation with PET. All nanocomposites showed about the same value for the peak heat release rate (PHRR). The amount of char increases after nanocomposite formation and this could account for the PHRRs. Copyright © 2006 John Wiley & Sons, Ltd.

KEYWORDS: poly(ethylene terephthalate) (PET); clay; nanocomposites; surfactants; melt blending

INTRODUCTION

The fact that clay particles can be dispersed in polymers has been well established[1] since the 1960s, but has gained substantial new momentum from the perspective of high performance composite materials in the last decade. A pioneering study that catalyzed this renewed research interest and perspective was by the Toyota research group who reported the preparation of a high performance polymer/layered-silicate nanocomposite (PLSN).[2–4] Since then the field has been actively pursued, mostly because of the opportunities for concurrent enhancements in mechanical, thermal, barrier and flammability properties[5–7] afforded by the ''addition'' of small amounts of clay. Typically, such property enhancements originate from the nanometer-scale dispersion of these highly anisotropic inorganic fillers in the polymer matrix, and thus appropriate organic modification of the inherently hydrophilic clays is a crucial point in the design and preparation of PLSNs. Among the modifiers used, quaternary ammonium surfactants are the most common because, aside from their low cost and commercial availability, they can render clays miscible with a broad range of polymer matrices.[6–8] The properties at the interface between the clay and the polymer are critical to an understanding of nanocomposite formation and this interface must be considered.[9,10]

Poly(ethylene terephthalate) (PET) finds application in a wide array of fields, both in fiber and non-fiber applications (such as packaging, electrical, automotive, constructions, electronics),[11] because it combines low cost with good chemical resistance and good spinnability.[12] Incorporation of nanodispersed clays in PET is not expected to impair these desirable attributes,[13] whereas it is expected to act as a heterogeneous nucleating agent—speeding up the overall crystallization rate and slightly increasing the crystalline fraction.[13–16] The fact that clay particles are impermeable is also expected to promote a decreased permeability of the PET/clay nanocomposite,[13,17–19] as is typically the case for most polymer/clay nanocomposite systems. Preparation of PET/clay nanocomposites though, presents a challenge: the processing temperature of PET, as well as the temperature at which these polymers are synthesized by polycondensation reactions, is about 280°C, well above the decomposition temperature of the ammonium surfactants customarily used as layered silicate organic modifications. This means that neither melt-blending, nor straight-forward *in situ* polymerization can be employed for PET and ammonium modified clays. Consequently, one can prepare PET/clay hybrids either by solution blending[20] (where an elevated temperature

**Correspondence to*: C. A. Wilkie, Department of Chemistry, Marquette University, PO Box 1881, Milwaukee, WI 53201, USA.
E-mail: charles.wilkie@marquette.edu
†8th International Symposium on Polymers for Advanced Technologies 2005 (PAT 2005), Budapest, 13–16 September, 2005, Part 1

is not required, hence ammonium-based surfactants can be used), or by employing clay-modifications with a higher thermal stability (that would allow both for *in situ* polymerization[12,21–23] and/or for direct melt blending with PET.[24]) Among such thermally stable surfactants, the most interesting are alkyl chain imidazolium[24] and phosphonium halides.[25,26] These cationic surfactants, when employed as modifiers for layered-silicate clay fillers, allow for direct melt blended PET nanocomposites, without requiring extensive modifications of the existing production facilities or the use of organic solvents (both of which would impede the industrial application of such an approach).

This work presents novel PET/clay nanocomposites based on two classes of high thermal stability organic modifications for the clay fillers, and comparisons between hybrids with three different clays. Specifically, the melt-blending preparation, the nanocomposite morphologies [studied by X-ray diffraction (XRD), and bright field transmission electron microscopy (TEM)] are reported, along with a thorough evaluation of their thermal and flammability properties [studied by cone calorimetry and thermogravimetric analysis (TGA)]. In light of previous work from this laboratory, showing that it may be possible to obtain intercalated nanocomposites using relatively low shear if the interlayer space is large enough,[27] a Brabender Plasticorder was used for melt blending instead of a twin-screw extruder customarily used for PET/clay nanocomposite preparation.

EXPERIMENTAL

Materials

The polymer used was a commercial-grade PET resin (Voridian Aqua WA314) with an intrinsic viscosity of 0.76, kindly provided by Voridian, Division of Eastman Chemical Company. The inorganic clays used in this study were montmorillonite, hectorite and magadiite, all initially in their sodium form. Montmorillonite was supplied by Southern Clay Products and hectorite was supplied by Elementis Specialitis. Preparation of pristine magadiite has been previously described by Garces *et al*.[28] Styrene monomer was purchased from the Aldrich Chemical Co., Inc. and was passed through an inhibitor-remover column prior to usage. Most other chemicals were also purchased from Aldrich (quinoline 98%, vinylbenzyl chloride 97%, lauryl acrylate 90%, benzoyl peroxide 97%, diethylether and tetrahydrofuran) and were used without further purification.

Instrumentation

XRD measurements were used to observe the intercalated structure of the silicates, and were performed in a Rigaku powder diffractometer with Cu source ($\lambda = 1.54$ Å), scanning 2θ from 1° to 10°, at a 0.1° step; generator tension was 50 kV at 20 mA. All XRD specimens were compression molded.

Bright field TEM images were obtained with a JEOL 1200 EXII microscope operated with an accelerating voltage of 80 kV, and equipped with a Tietz F224 digital camera. Ultrathin sections (70–100 nm) of the nanocomposites were obtained with a microtome (Leica Ultracut UCT) equipped with a diamond knife. The sections were transferred to carbon-coated copper grids (200-mesh). No heavy metal staining of sections prior to imaging was necessary, since the contrast between the layered silicate and the polymer matrix was sufficient.

TGA was performed on a SDT 2960 Simultaneous DTA-TGA unit from TA Instruments, under a constant nitrogen flow of 40 ml/min. The experiments were performed at a temperature ramping of 20°C/min from 100 to 600°C. All samples were run in triplicate and show good reproducibility; temperatures are considered accurate to ±4°C, while char remaining at 600°C is considered to be accurate to ±3%.

Cone calorimeter measurements were performed at an incident flux of 35 kW/mm^2, on an Atlas Cone 2 instrument using a cone shaped heater, according to ASTM E 1354. Exhaust flow rate was 24 l/sec and the spark was continued until the sample ignited. The specimens for cone calorimetry were prepared by the compression molding of the sample (about 30 g) into 3 mm × 100 mm × 100 mm square plaques. Typical results from cone calorimetry are reproducible to within ±10%.

Preparation of organic modifiers (surfactants) and organo-clays

The structures of the hexadecyl-quinolinium (Q16) bromide and of the vinylbenzyl-ammonium chloride-lauryl-acrylate copolymer (L-surfactant) are shown in Fig. 1. The preparation of Q16 and vinylbenzyl choride-lauryl acrylate (L-surfactant) was carried out according to literature procedures.[29,30]

The organic modification of the pristine montmorillonite (NaMMT), hectorite (NaHect) and magadiite (NaMag) was carried out under similar conditions for 3 clays and followed literature procedures,[29–31] affording ''lauryl'' and ''quinolinium'' modified clays, respectively (denoted hereafter as MMT-L, MMT-Q16, Hect-Q16, Mag-Q16).

Preparation of the PET/clay nanocomposites

All the nanocomposites in this work were prepared by melt blending in a Brabender plasticorder for 7 min at 280° C and 60 rpm. The inorganic clay loading was kept at 3 wt% for all the samples. However, considering the different cation exchange capacity of the three clays and the different molecular weight of the two surfactants, the modified clay (organo-clay) loading varied in the nanocomposites, as shown in Table 1. Unfilled PET samples were processed in the same fashion as the nanocomposites and were used as controls.

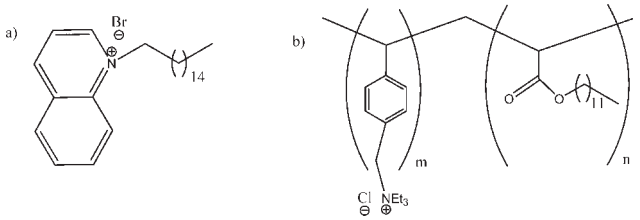

Figure 1. Structures of hexadecylquinolinium bromide (Q16) (a) and lauryl acrylate-vinylbenzyl triethylammonium chloride (L-surfactant) (b).

DOI: 10.1002/pat

Table 1. Compositions of PET/clay nanocomposites

Sample	PET (wt%)	Modified clay (wt%)	Inorganic (wt%)
PET	100	—	—
PET/MMT-L	88	12.0 (MMT-L)	3
PET/MMT-Q16	96.5	3.5 (MMT-Q16)	3
PET/Hect-Q16	96.5	3.5 (Hect-Q16)	3
PET/Mag-Q16	96	4.0 (Mag-Q16)	3

RESULTS AND DISCUSSION

Morphology of the PET/clay hybrids

Upon organic modification with the quinolinium surfactant, the *d*-spacing of the montmorillonite was expanded from 1.21 nm (NaMMT) to 1.73 nm (MMT-Q16). Subsequent melt blending of this organically modified MMT with PET, shifted the XRD diffraction peak to an even lower 2θ value, corresponding to a basal spacing of 3.15 nm (Fig. 2). The width of the XRD peak denotes that nanocomposite formation increased the disorder of the intercalated structures, suggesting that a mixed morphology, including immiscible, intercalated, and/or delaminated MMT structures, was probably obtained. This behavior is typical for MMT-based nanocomposite morphologies, given the lateral size distribution of MMT platelets. The lower magnification TEM micrograph (Fig. 3a) is representative of the nanocomposite structure, showing generally good clay dispersion of the MMT-Q16 in the polymer matrix, with no extended MMT agglomerates present. Tactoids are well dispersed throughout the polymer, most often separated by clay stacks of 2–4 layers and—to a smaller extent—single (exfoliated) MMT layers (Fig. 3b). This morphology is in concert with the XRD observation in Fig. 2, i.e. a broad, low-intensity d_{001} diffraction peak and a raised background.

A similar behavior can be seen in the case of PET/hectorite-Q16 (cf. Figs. 4 and 5). In the XRD, the basal spacing increased in this case from 1.18 nm for Na^+ hectorite to 1.73 nm for the hexadecyl-quinolinium modified hectorite and finally to 2.53 nm for the nanocomposite, denoting the formation of the intercalated morphology; once again the

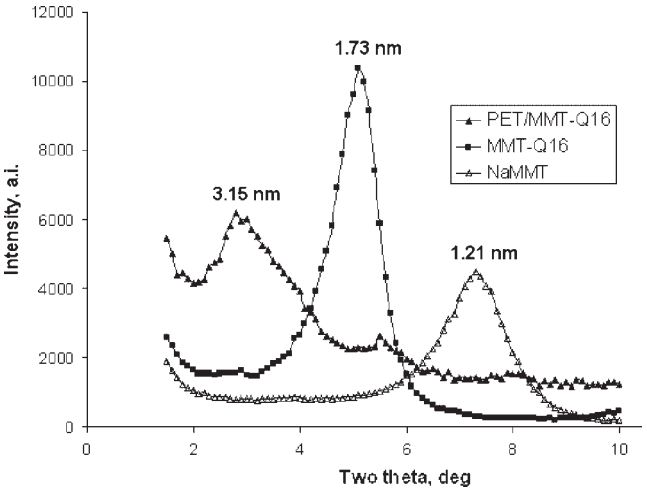

Figure 2. XRD trace of pristine and modified montmorillonite, along with its PET nanocomposite.

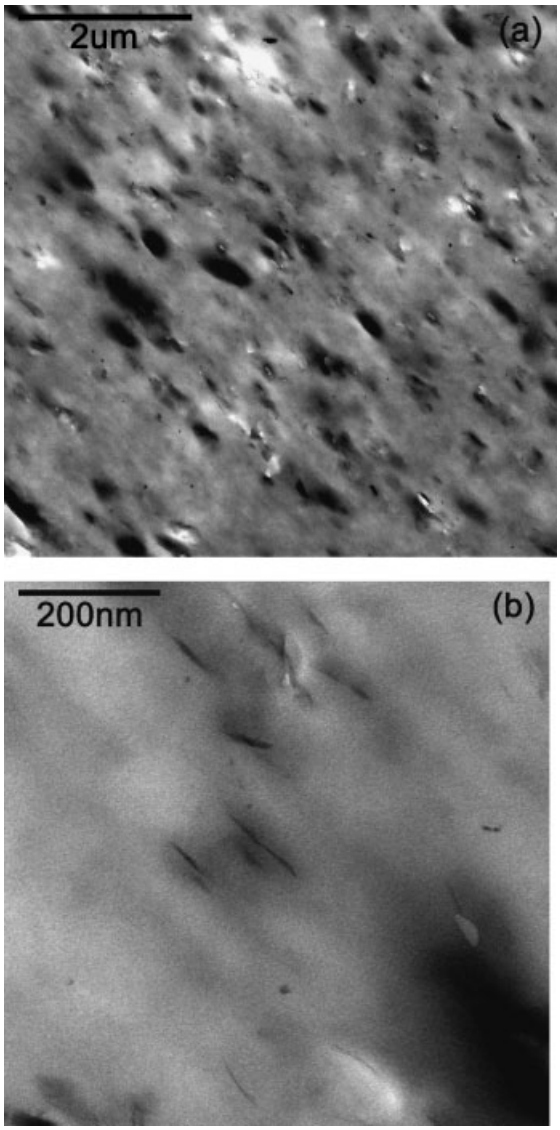

Figure 3. Bright field TEM micrographs of PET/MMT-Q16, low magnification (a) and higher magnification (b).

width of the XRD peak suggests that some disorder may have occurred. In the bright field TEM, the nanocomposite structure of the PET/Hect-Q16 (Fig. 5) is qualitatively the same as that of the PET/MMT-Q16 (Fig. 3), with well-dispersed tactoids throughout the PET matrix separated by 1–4 platelet stacks of organo-clay. Given the comparable platelet sizes of MMT and hectorite, the similar CEC values of the two silicates, and the common Q16 organic modification and nanocomposite processing, the very similar mesoscale nanocomposite structure is intuitively expected. However, it is interesting to note that the XRD d_{001} basal spacing of PET/hectorite did not increase as much as in the case of PET/montmorillonite, i.e. the d_{001} PET/Hect-Q16 spans the range of 4.4 to 1.8 nm (2θ spans 2°–5°) whereas for PET/MMT-Q16 d_{001} ranges from 4.4 to 2.2 nm (2θ spans 2°–4°). This small difference in basal spacing, i.e. PET seems to form wider and more disordered intercalated films between the MMT-Q16 platelets, could be associated with poorer dispersion in the Hect-Q16, which is also observed in comparing the low magnification TEM images of PET/Hect-Q16 (Fig. 5a) and PET/MMT-Q16 (Fig. 3a).

DOI: 10.1002/pat

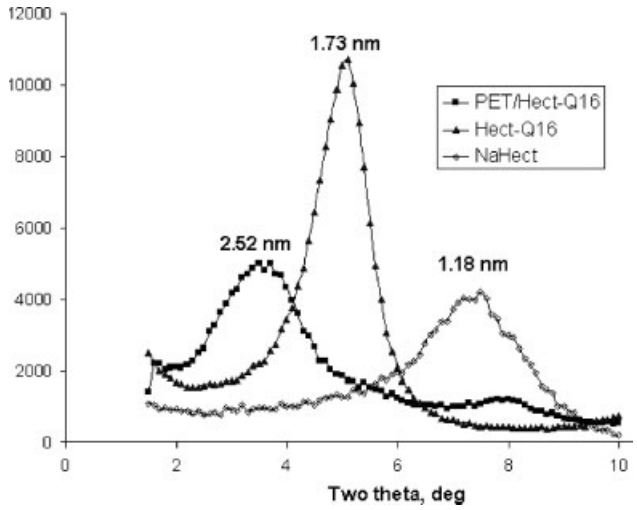

Figure 4. XRD trace of pristine and modified hectorite, along with its PET nanocomposite.

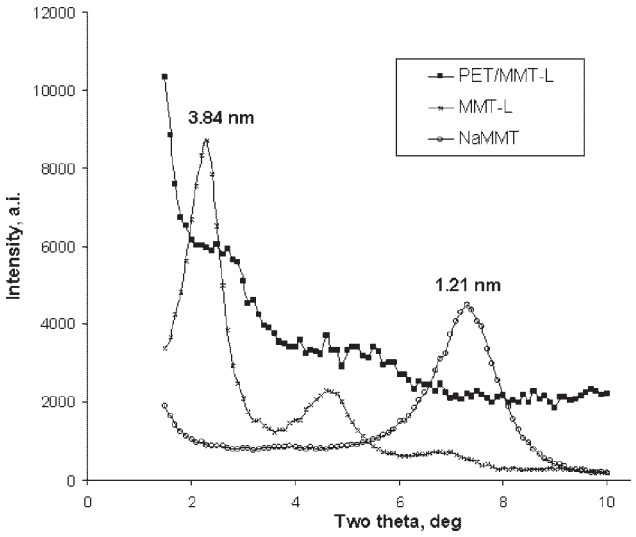

Figure 6. XRD trace of pristine and modified montmorillonite, along with its PET nanocomposite.

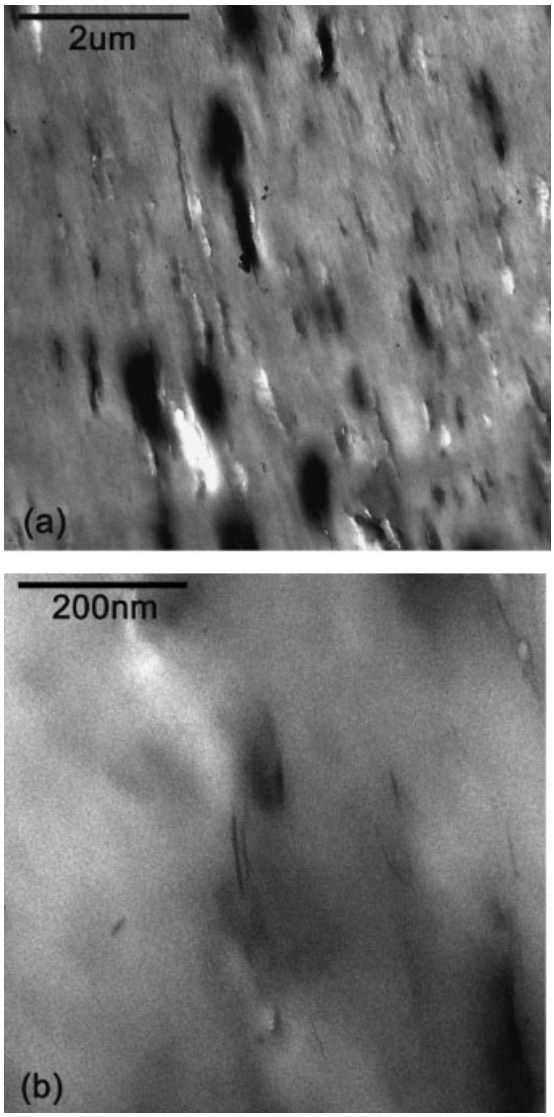

Figure 5. Bright field TEM micrographs of PET/Hect-Q, low magnification (a) and higher magnification (b).

A change in nanocomposite morphology occurs when PET is melt-blended with an oligomerically-modified MMT (MMT-L, cf. Figs. 6 and 7). In the XRD, there exists no definite peak for an intercalated d_{001} diffraction (Fig. 6), in contrast to the PET intercalated structures obtained for the quinolinium-modified clays. The 3.84 nm basal spacing of the MMT-L organo-clay is perhaps large enough that it may permit the delamination of the clay, or the formation of an intercalated structure characterized by a large enough d_{001} to be outside the wide-angle XRD detection limit (2θ below 1°). Moreover, the relatively large amount of oligomers introduced could act as a plasticizer or compatibilizer for the PET matrix, further facilitating the clay dispersion. The better dispersion is directly imaged in low magnification TEM (Fig. 7a), where much smaller and fewer tactoids are observed, compared to PET/MMT-Q16, and the vast majority of the silicate layers are in swollen stacks of 2–6 platelets. In addition, higher magnification images (Fig. 7b) clearly identify single platelets of clay and multi-layer assemblies with no periodic/parallel clay stacking, supporting the formation of a mostly delaminated nanocomposite.

In the case of the magadiite-based nanocomposite, the basal spacing of the pristine clay upon exchange with the Q16 surfactant increase from 1.52 nm to 1.63 nm, which is much smaller than the change in MMT and hectorite. For MMT and hectorite, the *d*-spacing increases by about 0.5 nm while in magadiite, the change is only 0.1 nm. As previously noted, an expanded interlayer distance helps to permit the entry of polymer between the clay layers and the change for magadiite may not be sufficient to enable the nano-dispersion of the clay in the polymer.[27] This is in agreement with the observation that upon melt blending with PET, the peak seems to decrease for the resulting PET/Mag-Q hybrid; this decrease in d_{001} is accompanied by a strong broadening and intensity depression, suggesting the formation of a microcomposite (no intercalated PET). In concert, low magnification TEM (Fig. 8a) shows poor dispersion characterized by relatively large and well-separated magadiite clusters and very few, if any, exfoliated fillers; the mesoscale

DOI: 10.1002/pat

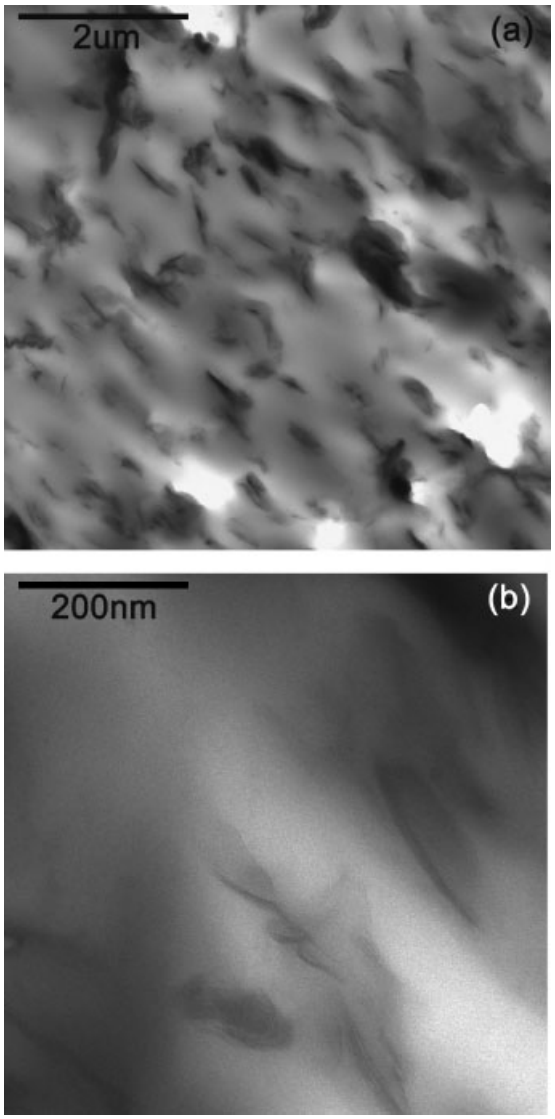

Figure 7. Bright field TEM micrographs of PET/MMT-L, low magnification (a) and higher magnification (b).

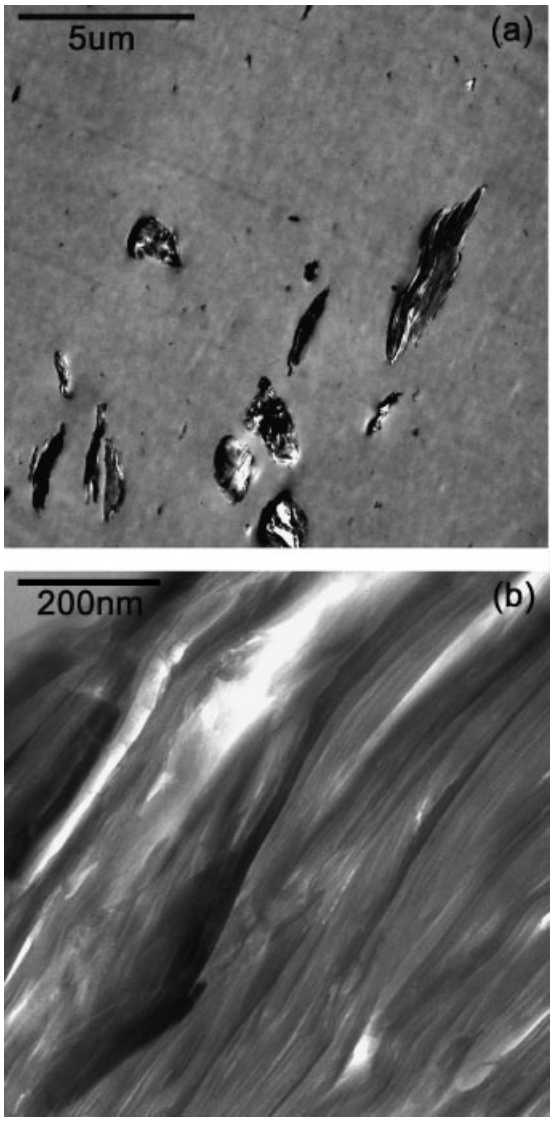

Figure 8. Bright field TEM micrographs of PET/Mag-Q16, low magnification (a) and higher magnification (b).

(micrometer) nanocomposite structure is characterized by lower filler dispersion than the respective MMT and Hect based PET hybrids. At higher magnification (Fig. 8b) the presence of stacked magadiite layers within the tactoids is apparent; compared to PET/MMT and PET/Hect hybrids, these structures contain much larger numbers (a few tens) of platelets per stack, and poorer parallel registry between successive layers. These TEM observations are in good agreement with structures that correspond to the XRD of Fig. 9 and this composite shows substantially lower nano dispersion than the MMT and Hect based hybrids and a mesoscale structure characteristic of a conventional—micro-composite—filled PET. The composite structure of PET/Mag-Q could be described as a mixed immiscible-intercalated morphology.

Thermal stability and fire retardancy evaluation of the PET/clay nanocomposites

The TGA curves of the four organically-modified clays are presented in Fig. 10. With the exception of Mag-Q16, all the modified clays showed remarkable thermal stability, the mass loss at 300°C being less than 2%, which allows for them to be melt-blended with high processing temperature polymers like PET. Moreover, up to 320°C, their thermal behavior is comparable to an imidazolium-based clay

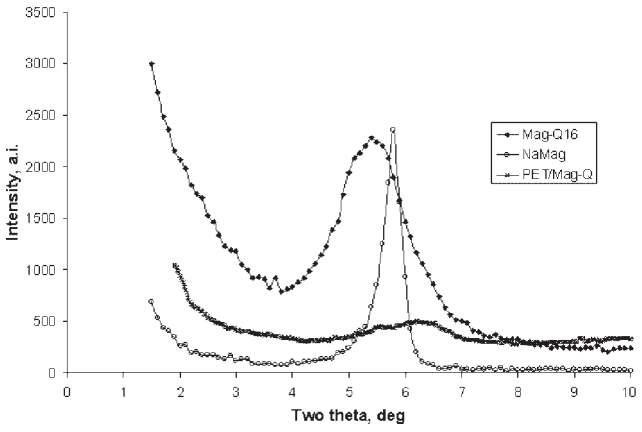

Figure 9. XRD trace of pristine and modified magadiite, along with its PET nanocomposite.

DOI: 10.1002/pat

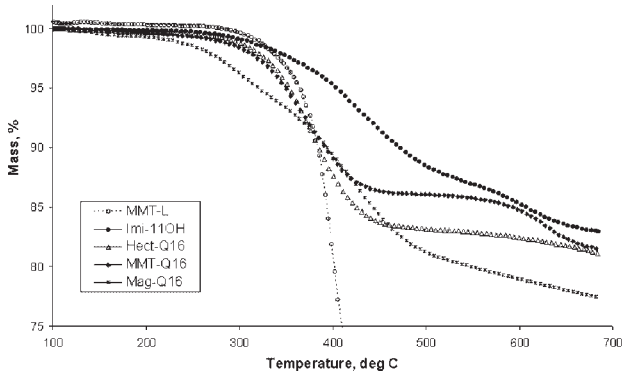

Figure 10. TGA curves for the modified clays (nitrogen atmosphere).

(e.g. MMT exchanged with 1-(11-hydroxy-undecyl)-2,3-dimethyl-3*H*-imidazol-1-ium), but above this temperature the imidazolium clay outperforms the respective quinolinium and lauryl clays. The thermal stability behavior of the organo-clays is also summarized in Table 2 through the temperatures at 2% and 5% mass loss, and the char yield at 600°C.

Comparing now the TGA behavior of PET and the various PET nanocomposites (Fig. 11) with the organo-clays of Fig. 10, it is seen that for PET/Hect-Q16, PET/Mag-Q16 and PET/MMT-Q16 the temperature of 10% mass loss ($T_{0.1}$) is virtually unchanged compared to virgin PET (420°C), while for PET/MMT-L it decreased by 15°C. Considering that the oligomeric part of the surfactant used for clay modification makes up about 9% of the composite, this behavior should be expected. When comparing the temperature of 50% mass loss ($T_{0.5}$) no marked change is observed between the pure polymer and its nanocomposites; the presence of the clay appears to have no marked influence. It is interesting to note that the addition of clay greatly improved the amount of char at 600°C, from 5% in the case of virgin PET to more than 15% for the nanocomposites studied, all containing 3% of inorganic filler. The amount of char does not seem to depend either upon the surfactant or upon the type of clay used, since the same amount of char was obtained in all the cases. Apparently some of the polymer does not undergo thermal degradation upon nanocomposite formation.

The cone calorimetry results, as shown in Table 3, are typical for polymer/inorganic nanocomposites. Even though the total heat released is unchanged for PET and its nanocomposites, the peak heat release rate (PHRR) is significantly reduced when compared to virgin PET at the

Table 2. Temperatures corresponding to 2 and 5% mass loss along with the fraction of char (%) at 600°C for the all the organically-modified clays used in this study

Clay	$T_{0.02}$ (°C)	$T_{0.05}$ (°C)	Char at 600°C (%)
MMT-L	334	366	26
Hect-Q16	320	351	82
MMT-Q16	310	350	85
Mag-Q16	264	319	79
Imi-11OH	338	403	85

$T_{0.02}$ = temperature at 2% mass loss; $T_{0.05}$ = temperature at 5% mass loss.

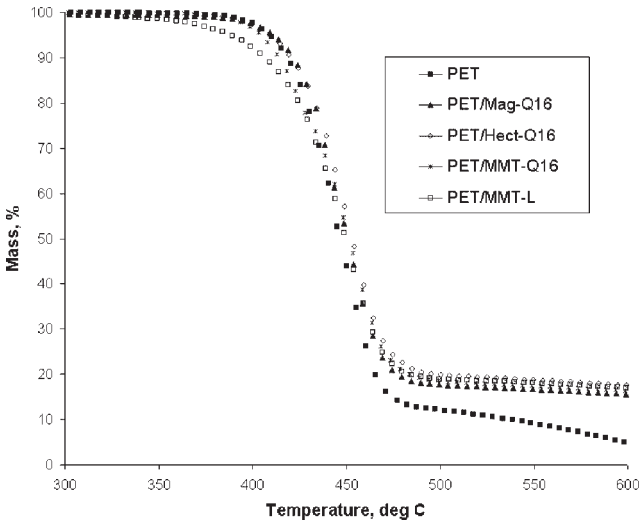

Figure 11. TGA curves for the PET/clay nanocomposites.

same thickness (3 mm). It should be noted that the 3 mm thick samples of PET are apparently thermally thin, since burning of 6 mm thick samples in the cone gives a significantly lower value for the PHRR, 574 kW/m^2. The appearance of the heat release rate (HRR) curves for the nanocomposites suggests that they are thermally thick. In this paper, comparisons are made between the 3 mm thick samples in all cases. The mass loss rates are approximately constant for the three montmorillonite systems but the value is significantly lower for magadiite. There is only a slight increase in the average specific extinction area (ASEA) of PET nanocomposites (20% at the largest) as compared to virgin PET. The prolonged burning time of nanocomposites can be observed from the shape of the HRR curves shown in Fig. 12, along with the decrease in the time-to-ignition (t_{ig}).

It is noteworthy that magadiite-based PET ''nanocomposites'' give the same PHRRs as the other systems studied here. In previous studies, polystyrene/magadiite nanocomposites[31] and vinyl-ester/magadiite systems[32] have been studied and in each case the PHRRs are much higher than those obtained when montmorillonite was used. A large reduction in PHRR is usually associated with nanocomposite formation in either a delaminated or intercalated morphology. The reductions in PHRR are roughly comparable for all four nanocomposites yet the morphology, as assigned by XRD and TEM, varies from very good nanoscale

Table 3. Cone calorimetry measured properties (PHRR, THR, AMLR, T_{ig} and ASEA) for unfilled PET and its nanocomposites

Composition	PHRR (kW/m^2)	THR (MJ/m^2)	AMLR (g/sm^2)	t_{ig}(sec)	ASEA[e] (M^2/kg)
PET	1323 ± 98	53 ± 8	35.4 ± 0.4	92 ± 7	425 ± 34
PET/MMT-L	734 ± 45	63 ± 6	29.2 ± 0.3	81 ± 5	506 ± 42
PET/MMT-Q16	680 ± 34	52 ± 2	29.6 ± 0.4	71 ± 6	535 ± 23
PET/Hect-Q16	696 ± 15	51 ± 2	31.2 ± 0.4	61 ± 5	455 ± 33
PET/Mag-Q16	645 ± 22	46 ± 6	19.3 ± 0.6	62 ± 6	416 ± 28

Note: PHRR, peak heat released rate; THR, total heat released; AMLR, average mass loss rate; t_{ig}, time to ignition; ASEA, average specific extinction area.

DOI: 10.1002/pat

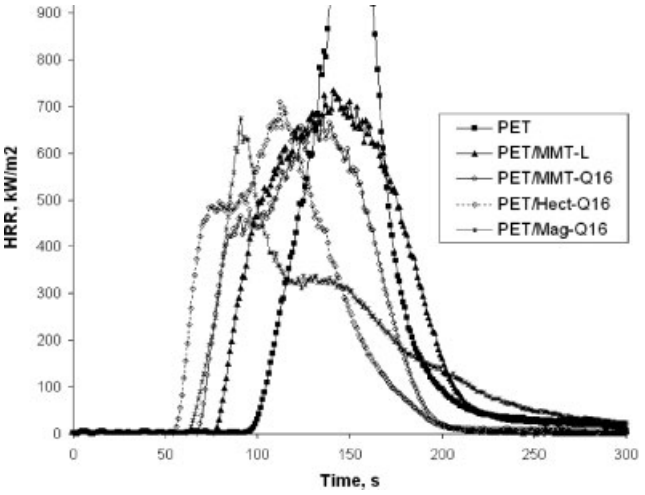

Figure 12. HRR curves of PET and PET nanocomposites.

and mesoscale dispersion for PET/MMT-L, to good for MMT-Q16 and Hect-Q16, to rather poor nanoscale dispersion and conventional-like mesoscale dispersion for Mag-Q16. Comparing these three systems, all showing similar PHRR values despite the clear difference in composite morphologies, as measured by XRD and TEM, raises the question of how closely the assigned morphology is representative of the nanocomposite, and also points out the need for additional measurements of morphology (e.g. scattering). Nevertheless, given the significantly improved amount of char produced at 600°C by all PET/modified clay systems (as observed from TGA data), it is very tempting to correlate the PHRR values and the increased char formation. Since there is no essential difference in the char yield, regardless of the nano-dispersion of the PET/modified clay nanocomposites, the similar cone results seem to be consistent with this assumption.

The difference in the flammability effect upon composite formation between magadiite/polystyrene, magadiite/vinyl-ester and magadiite/PET is very interesting and requires further comment. Two possibilities may be suggested to explain this difference: either the nano-dispersion of magadiite in PET is better than that with the other two polymers, or the quinolinium surfactant—used here as the organic modification of magadiite—is more effective in FR improvement than those previously used. Further investigations are required to answer this question.

CONCLUSIONS

PET/layered-silicate nanocomposites can be prepared by melt blending in a Brabender plasticorder using lauryl-oligomers and quinolinium-based surfactants. The nanocomposite morphologies obtained range from very good nanoscale dispersions (mostly-delaminated nanocomposites) to rather poor dispersions (conventional microcomposite) depending on the nature of the filler and the surfactant. In all the cases, and despite the difference in morphology, the PHRRs are constant, which may be correlatable to the improved char formation.

REFERENCES

1. Theng BKG. *Formation and Properties of Clay-Polymer Complexes*. Elsevier: Amsterdam, 1970; and references therein.
2. Usuki A, Kojima Y, Kawasumir M, Okada A, Kurauchi T, Kamigaito O. Swelling behavior of montmorillonite cation exchanged for ω-amino acids for ε-caprolactam. *J. Mater. Res.* 1993; **8**: 1174–1178.
3. Usuki A, Kojima Y, Kawasumi M, Okada A, Fukushima Y, Kurauchi T, Kamigaito O. Synthesis of nylon 6-clay hybrid. *J. Mater. Res.* 1993; **8**: 1179–1184.
4. Kojima Y, Usuki A, Kawasumi M, Okada A, Fukushima Y, Kurauchi T. Mechanical properties of nylon 6-clay hybrid. *J. Mater. Res.* 1993; **8**: 1185–1189.
5. Okada A, Usuki A. The chemistry of polymer-clay hybrids. *Mater Sci. Eng. C* 1995; **C3**: 115.
6. Giannelis EP, Krishnamoorti RK, Manias E. Polymer-silicate nanocomposites. *Adv. Polym. Sci.* 1998; **138**: 107–148.
7. Alexander M, Dubois P. Polymer-layered silicate nanocomposites: Preparation, properties and uses of a new class of materials. *Mater. Sci. Eng. R* 2000; **28**: 1–63.
8. Ray SS, Okamoto M. Polymer/layered silicate nanocomposites: A review from preparation to processing. *Prog. Polym. Sci.* 2003; **28**: 1539–1641.
9. Keszei S, Matkó Sz, Bertalan Gy, Anna P, Marosi Gy, Tóth A. Progress in interface modifications: from compatibilization to adaptive and smart interphases. *Eur. Polym. J.* 2005; **41**: 697–705.
10. Szep A, Szabo A, Toth N, Anna P, Marosi Gy. Role of montmorillonite in flame retardancy of ethylenevinyl acetate copolymer. *Polym. Degrad. Stab.* 2006; **91**: 593–599.
11. Margolis J. In *Engineering Thermoplastics. Properties and Applications*, Margolis J (ed.). Marcel Dekker: New York, 1985; 1–19.
12. Chang J-H, Kim SJ, Joo YL, Im S. Poly(ethylene terephthalate) nanocomposites by *in situ* interlayer polymerizarion: the thermo-mechanical properties and morphology of the hybrid fibres. *Polymer* 2004; **45**: 919–926.
13. Pinnavaia TJ, Beall GW (eds). *Polymer-Clay Nanocomposites*. John Wiley & Sons;2000: chapters 9 and 11.
14. Wang T, Chen L, Chua YC, Lu X. Crystalline morphology and isothermal crystallization kinetics of poly(ethylene terephthalate)/clay nanocomposites. *J. Appl. Polym. Sci.* 2004; **94**: 1381–1388.
15. Phang P, Liu H. Crystallization and melting behavior of polyester/clay nanocomposites, *Polym. Int.* 2004; **53**: 1282–1289.
16. Nakajima H, Manias E. PET/montmorillonite nanocomposites prepared by direct melt-blending, in preparation.
17. Qureshi N, Stepanov EV, Schiraldi D, Hiltner A, Baer E. Oxygen-barrier properties of oriented and heat-set poly (ethylene terephthalate). *J. Polym. Sci., Part B: Polym. Phys.* 2000; **38**: 1679.
18. Nielsen LE. Models for the permeability of filled polymer systems. *J. Macromol. Sci. (Chem.) A* 1967; **1**: 929–942.
19. Liu W, Tian X, Cui P, Li Y, Zheng K, Yang Y. Preparation and characterization of PET/silica nanocomposites. *J. Appl. Pol. Sci.* 2004; **91**: 1229–1232.
20. Ou CF, Ho MT, Ling JR. Synthesis and characterization of poly(ethylene terephthalate) nanocomposites with organo-clay. *J. Appl. Polym. Sci.* 2004; **91**: 140–145.
21. Wu D, Chen F, Li R. Reaction kinetics and simulations for solid-state polymerization of poly(ethylene terephthalate). *Macromolecules* 1997; **30**: 6737–6742.
22. Imai Y, Nishimura S, Abe E, Tateyama H, Abiko A, Aoyama T, Taguchi H. High-modulus poly(ethylene terephthalate)/expandable fluorine mica nanocomposites with a novel reactive compatibilizer. *Chem. Mater.* 2002; **14**: 477–479.
23. Imai Y, Inukay Y, Tateyama H. Properties of poly(ethylene terephthalate)/layered silicate nanocomposites prepared by two-step polymerization procedure. *Polym. J.* 2003; **35**(3): 230–235.
24. Davis CH, Mathias LJ, Gilman JW, Schiraldi DA, Shields JR, Trulove P, Sutto TE, Delong HC. Effects of melt-processing conditions on the quality of poly(ethylene terephthalate) montmorillonite clay nanocomposites. *J. Polym. Sci., Part B; Polym. Phys.* 2002; **40**: 2661–2666.
25. Zhu J, Uhl FM, Morgan AB, Wilkie CA. Studies on the mechanism by which the formation of nanocomposites

DOI: 10.1002/pat

enhances thermal stability. *Chem. Mater.* 2001; **13**(12): 4649–4654.
26. Zhu J, Morgan AB, Lamelas FJ, Wilkie CA. Fire properties of polystyrene-clay nanocomposites. *Chem. Mater.* 2001; **13**: 3774–3780.
27. Jang BN, Wang D, Wilkie CA. Relationship between the solubility parameter of polymers and the clay dispersion in polymer/clay nanocomposites and the role of the surfactant. *Macromolecules* 2005; **38**: 6533–6543.
28. Garces JM, Lakso SR, Schoeman BJ, Ulmer DC. Patent Application WO 01/83370 A2.
29. Chigwada G, Wang D, Wilkie CA. Polystyrene nanocomposites based on quinolinium and pyridinium surfactants. *Polym. Degrad. Stab.* 2006; **91**: 848–855.
30. Zhang J-, Jiang DD, Wilkie CA. Polyethylene and polypropylene nanocomposites based upon an oligomerically modified clay. *Thermochim. Acta* 2005; **430**: 107–113.
31. Wang D, Jiang DD, Pabst J, Han Z, Wang J, Wilkie CA. Polystyrene magadiite nanocomposites. Polym. *Eng. Sci.* 2004; **44**: 1122–1131.
32. Chigwada G, Jash P, Jiang DD. Wilkie CA. Fire retardancy of vinyl ester nanocomposites: synergy with phosphorus-based fire retardants. *Polym. Degrad. Stab.* 2005; **89**: 85–100.

DOI: 10.1002/pat